Electrochemical deposition and characterization of zinc–nickel alloys deposited by direct and reverse current

JELENA B. BAJAT[1*#], ALEKSANDRA B. PETROVIĆ[2] and MIODRAG D. MAKSIMOVIĆ[1]

[1]*Faculty of Technology and Metallurgy, University of Belgrade, Karnegijeva 4, P. O. Box 3503, 11120 Belgrade (e-mail: jela@elab.tmf.bg.ac.yu) and* [2]*Krušik akumulatori a.d., 14000 Valjevo, Serbia and Montenegro*

Abstract: Zn–Ni alloys electrochemically deposited on steel under various deposition conditions were investigated. The alloys were deposited on a rotating disc electrode and on a steel panel from chloride solutions by direct and reverse current. The influence of reverse plating variables (cathodic and anodic current densities and their time duration) on the composition, phase structure and corrosion properties were investigated. The chemical content and phase composition affect the anticorrosive properties of Zn–Ni alloys during exposure to a corrosive agent (3 % NaCl solution). It was shown that the Zn–Ni alloy electrodeposited by reverse current with a full period $T = 1$ s and $r = 0.2$ exhibits the best corrosion properties of all the investigated alloys deposited by reverse current.

Keywords: Zn–Ni alloy, electrodeposition, reverse current, ALSV, corrosion.

INTRODUCTION

Among a variety of types of coating, zinc coating is widely used as a protective coating on steel and one of the most important problems in galvanizing is the improvement of the protective and functional properties of Zn coatings. According to the literature,[1–3] zinc alloys can provide improved corrosion resistance compared to pure zinc in the protection of ferrous-based metals. This is easily achieved by alloying Zn with more noble metals, mostly with metals of the iron group (Ni, Co and Fe).[4,5] Among them, zinc–nickel alloys are mostly used because of their high degree of corrosion resistance and good mechanical properties.[6–9] Zn–Ni alloys with a Ni content in the range of 12–14 wt.% exhibit the best corrosion properties and can be several times better than a pure zinc coating of the same thickness.[10] Zinc–nickel alloys exist in various phases and their structure and morphology also determine the corrosion resistance of a deoposit.[11,12]

---

*   Author for correspondence.

\#   Serbian Chemical Society active member.

It is well known that the application of periodically changing currents (pulse current, reverse current, *etc*.) in plating leads to improvements in the quality of electrodeposits: smooth deposits are achieved, with decreased porosity, better ductility and hardness, as well as control of the deposit composition.[13,14]

In this study an attempt was made to determine reverse plating parameters that would lead to a Zn–Ni alloy with the best corrosion resistance being obtained. The variables used in reverse plating (RC) are: cathodic current density (j_c), anodic current density (j_a), and their time duration, t_c and t_a, respectively. In an earlier work,[15] the corrosion properties of Zn–Ni deposits obtained from chloride and sulphate plating solutions using various current densities were examined, and the alloy obtained from a chloride bath at 20 mA cm^{-2} at 40 ºC showed the best corrosion properties. This current density was chosen as the average current density (j_{av}) in the reverse plating in this work. The influence of other variables on the chemical composition, phase structure and corrosion properties of the obtained Zn–Ni alloys was investigated.

EXPERIMENTAL

Zn–Ni alloys were electrodeposited on a steel panel or on a rotating disc electrode from a chloride bath:[16] 15 g dm^{-3} ZnO, 60 g dm^{-3} NiCl$_2$·6H$_2$O, 250 g dm^{-3} NH$_4$Cl and 20 g dm^{-3} H$_3$BO$_3$ at 40 ºC and pH 6.0. The electrolytes used were prepared using p.a. chemicals and double distilled water. The working electrode was: a) a Pt rotating disc electrode (RDE) (d = 8 mm, at 2000 rpm), for the determination of the phase structure and chemical analysis, and a steel plate (20 mm × 20 mm × 0.25 mm), for the determination of the current efficiency and corrosion measurements. Prior to each electrodeposition, the Pt disc surface was mechanically polished with a polishing cloth (Buehler Ltd.), impregnated with a water suspension of alumina powder (0.3 μm grade), and then rinsed with pure water in an ultrasonic bath. The test panels were pretreated by mechanical cleaning (polishing successively with emery papers of the following grades: 280, 360, 800 and 1000) and then degreased in a saturated ethanolic solution of sodium hydroxide, pickled with a 1 : 1 hydrochloric acid solution for 30 s and finally rinsed with distilled water. The counter electrode was either a Ni spiral wire, placed parallel to the RDE at a distance of 1.5 cm, or platinized titanium, placed parallel to the steel electrode at a distance of 1.5 cm.

TABLE I. The reverse current parameters used in the first set of experiments; r = 0.5

T/s	0.1	0.2	1	2	3	10	20
t_a/s	0.033	0.067	0.33	0.67	1.0	3.3	6.7
t_c/s	0.067	0.133	0.67	1.33	2.0	6.7	13.3

TABLE II. The reverse current parameters used in the second set of experiments; T = 1 s

r	0.83	0.67	0.50	0.40	0.33	0.20
t_a/s	0.45	0.40	0.33	0.28	0.25	0.17
t_c/s	0.55	0.60	0.67	0.72	0.75	0.83
j_A/mA cm^{-2}	215	145	60.0	46.7	40.0	30.0

Zn–Ni alloys were deposited galvanostatically at constant current, j_{DC} = 20 mA cm^{-2}, and at reverse current with an average current density of j_{av} = 20 mA cm^{-2}. The two sets of experiments were

carried out using reverse current plating. In the first set, the full period of the RC wave, T $(T = t_a + t_c)$ was varied, while the ratio of the anodic and cathodic time duration, r $(r = t_a / t_c)$ was kept constant at r = 0.5 (Table I). In the second set, the values of r were varied at a constant value of $T = 1$ s (Table II).

For the determination of their phase structure, the alloys were dissolved using anodic linear sweep voltammetry (ALSV). The alloys were dissolved at room temperature (23 ± 1 °C) with a sweep rate of 1 mV s^{-1} and a rotation of 2000 rpm in N_2 saturated 0.5 mol dm^{-3} Na_2SO_4 + 0.05 mol dm^{-3} EDTA solution. The counter electrode used in these experiments was a Pt-spiral wire and the reference electrode was a saturated calomel electrode (SCE). All potentials are referred to the SCE.

The chemical composition of the Zn–Ni alloy was determined by atomic absorption spectroscopy using a Perkin Elmer AAS-1100 spectrophotometer.

The current efficiency was calculated on the basis of the chemical composition and the Faraday law.

All experiments were carried out using EG & G Princeton Applied Research potentiostat-galvanostats, Model 273A, Model 175 and Model 173 and a Pine Instrument Company rotator, model AFASR.

RESULTS AND DISCUSSION

Chemical composition

The Ni content in the Zn–Ni deposits as a function of the RC wave period, T, and of the ratio of the anodic and cathodic current, r, are shown in Figs 1 and 2, respectively. It can be seen from Fig. 1 that the Ni content increases with increasing T, which could be explained by more intense Zn dissolution, being the less noble alloy component, during the anodic period, t_a.
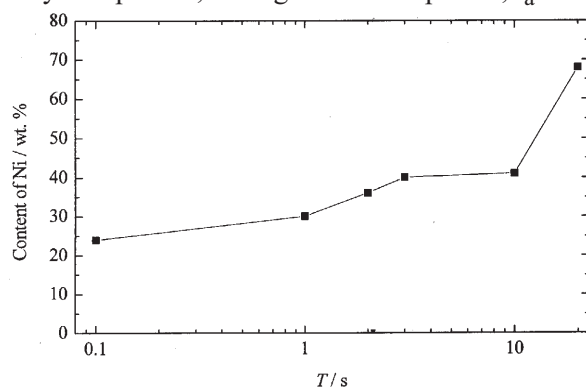

Fig. 1. The dependence of the Ni content in the alloy on different reverse current wave periods, at a constant r value of 0.5.

The increase of the Ni content shown in Fig. 2 could be explained similarly, namely, an increase of r refers to an increase of the duration of the anodic time during which Zn, as the less noble alloy component, dissolves to a greater extent, thus leading to an increase of the Ni content in the Zn–Ni alloy with increasing r.

The effect of anodic dissolution charge during one RC wave period ($T = 1$ s), Q_a, for different values of r, on the Ni content in the alloy is shown in Fig. 3. It can be seen from Fig. 3 that this dependence follows a straight line and that the Ni content increases with increasing Q_a. According to the literature, Zn–Ni alloys with a Ni content in the range of 12–14 wt.% exhibit the best corrosion properties,[3] hence, it can be concluded that Zn–Ni alloys with this beneficial Ni content could not be obtained by reverse plating with $T = 1$ s and $r > 2$.
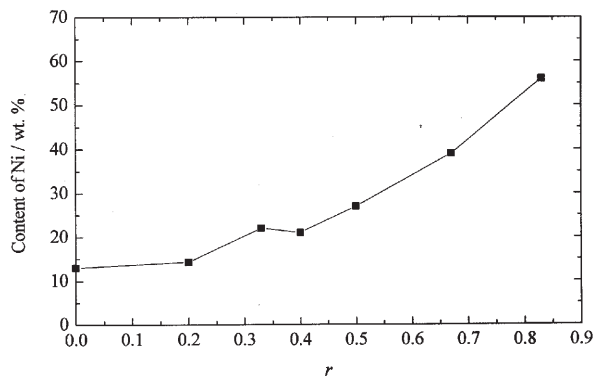
BAJAT, PETROVIĆ and MAKSIMOVIĆ

Fig. 2. The dependence of the Ni content in the alloy on the *r* value, with a constant *T* value of 1s (*r* = 0 – direct plating).
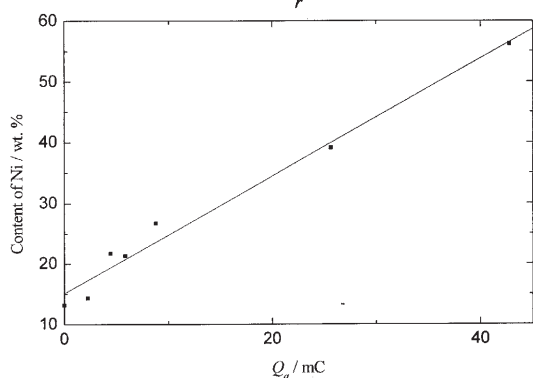

Fig. 3. The dependence of the Ni content in the alloy on the anodic dissolution charge during one RC wave period.
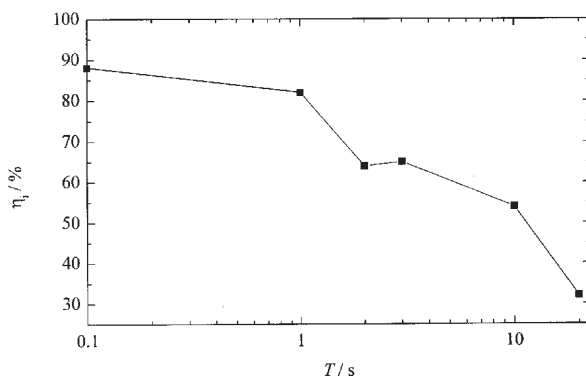

Fig. 4. The dependence of the current efficiency on different reverse current wave periods, *T*, for a constant *r* value of 0.5 on a RDE.

The current efficiency

The current efficiency was determined in three different ways: on the basis of the results obtained from chemical analysis and the Faraday law; from the weight of the alloy, determined from the weight difference between the steel plate before and after alloy plating, and from the ratio of the anodic dissolution charge, Q_a (determined under ALSV curves), and the deposition charge, determined from the average current density, j_{av}, and the overall deposition time.

The influence of the reverse current parameters on the current efficiency determined from chemical analysis is shown in Figs. 4 and 5. The current efficiency
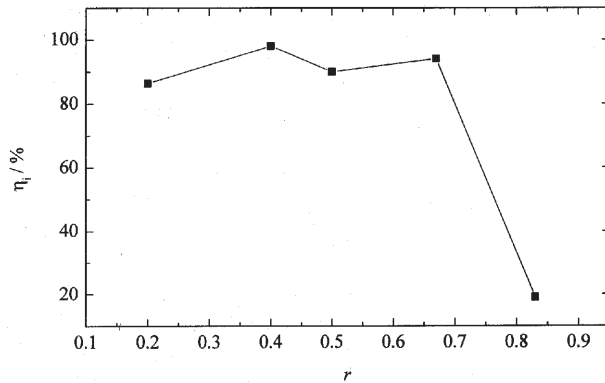
Fig. 5. The dependence of the current efficiency on the r value, for a constant T value of 1 s on a RDE.

decreases with increasing RC wave period, T (Fig. 4). The time duration of anodic dissolution, t_a, increases with increasing T (at a constant r value) and during this anodic time period Zn, as the less noble element, preferably dissolves, the Zn–Ni alloy becomes enriched in Ni and during the following cathodic period of alloy deposition, t_c, hydrogen evolves at a higher rate (the overpotential of hydrogen evolution is smaller on Ni than on Zn)[17], and this leads to a smaller current efficiency.

The decrease of the current efficiency with increasing r, shown in Fig. 5, could be explained likewise: a larger value of r (at constant T) corresponds to a larger value of t_a during which Zn preferably dissolves, leading to more intense hydrogen
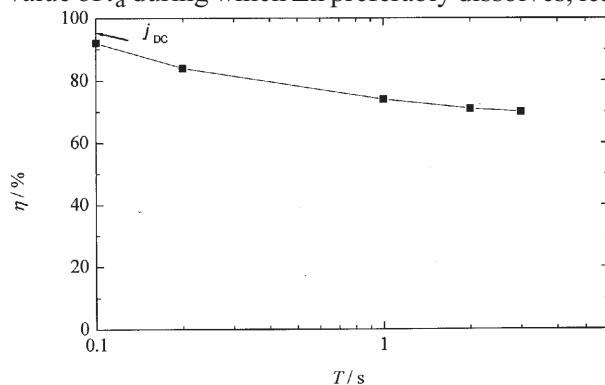

Fig. 6. The dependence of the current efficiency on different reverse current wave periods, T, for a constant r value of 0.5, on steel plates.
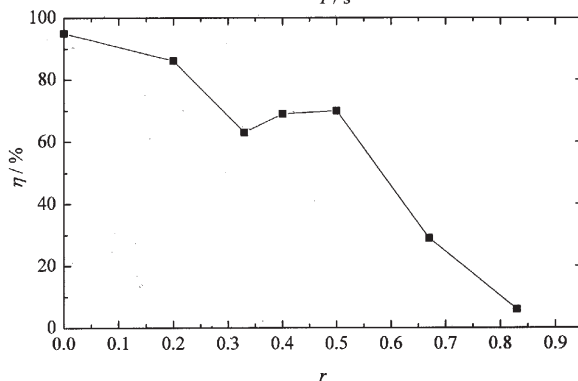

Fig. 7. The dependence of the current efficiency on the r value, for a constant T value of 1 s, on steel plates.
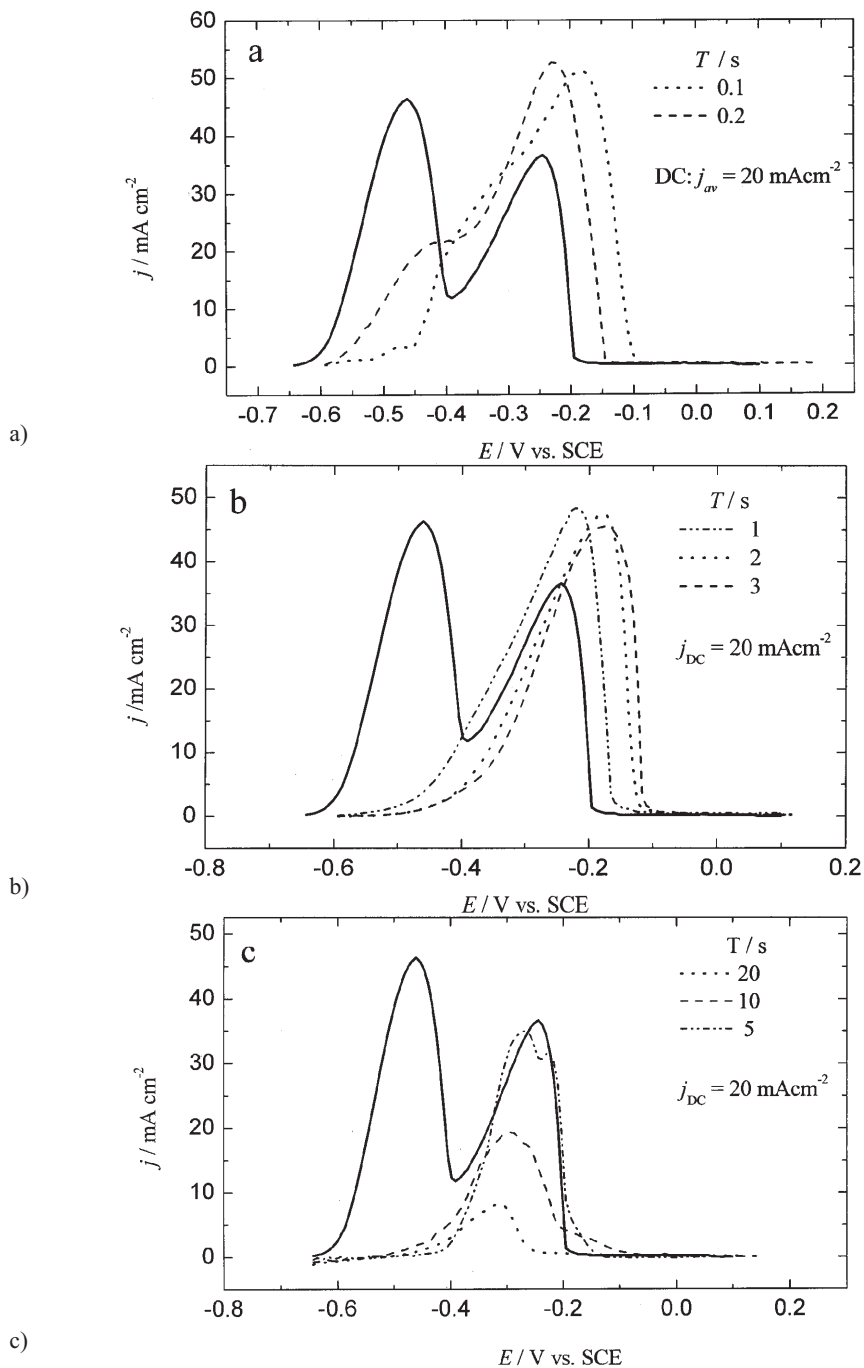
a)

b)

c)

Fig. 8. ALSVs in Na_2SO_4 + EDTA solution of the dissolution of Zn–Ni alloys, deposited by DC and RC with different reverse current wave periods, T, at a constant r value of 0.5.
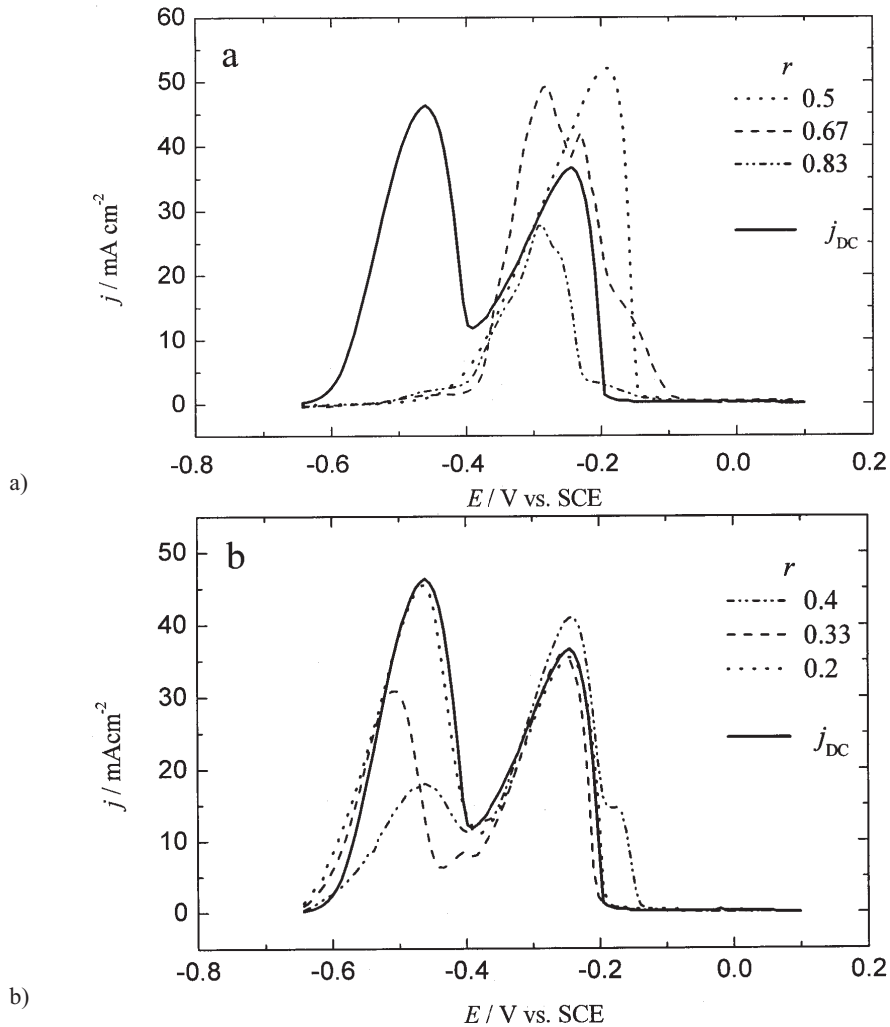
Fig. 9. ALSVs in Na_2SO_4 + EDTA solution of the dissolution of Zn–Ni alloys, deposited by DC and RC with different r values at a constant T value of 1 s.

evolution during the following cathodic time, t_c and, consequently, resulting in a decrease in the current efficiency.

Figs. 6 and 7 show the dependence of the current efficiency, η_i, on the reverse current parameters, T and r, for Zn–Ni alloys deposited on steel panels, respectively. The decrease in the current efficiency with increasing T, or r, can also be seen in these figures. During the anodic period of time in reverse current alloy plating, iron partially dissolves from the steel panel, and, consequently, during the cathodic period it is deposited on, or incorporated in the alloy as a hydroxide (which could be seen from the color of the deposit). Hence, the values of the current efficiency obtained in this maner could not be used as relevant values.

In Zn–Ni alloys obtained with RC with constant r ($r = 0.5$) and T values of 5, 10 and 20 s, cracks appeared over the entire alloy surface and the adhesion was poor, hence such deposits were not considered for the determination of the current efficiency. However, under the same deposition conditions for plating on a RDE, more compact deposits were obtained, hence the appearance of the alloys deposited on steel panels could be related to the presence of Fe. This is in agreement with literature data[18] according to which the presence of iron in the electrolyte (at a concentration of several ppms) results in cracked deposits.

Alloy phase structure

Despić and coworkers[19–21] showed that the method of anodic linear sweep voltammetry (ALSV) could be used for the qualitative and quantitative determination of the phase structure of some alloys. When an alloy film is polarized anodically under potentiodynamic conditions, the components will dissolve at various potentials, depending on their equilibrium and kinetic properties. When the activity of a component in a phase is reduced to zero, a dissolution current peak will be produced. Various phase structures and chemical forms present in an alloy will produce various current peaks. Therefore, the peak structure obtained is characteristic for components of an alloy and the phase structure of the deposit.[22] Very important results concerning the deposition of Zn–Ni alloys and their phase characterization were published by Swathirajan.[11,12]

The phase structure was investigated in Na_2SO_4 solution containing complex forming ions, in the presence of which a Zn–Ni alloy completely dissoslves. Namely, it is well known[23] that pure Zn dissolves but zinc alloys do not dissolve in Na_2SO_4 solution, while in the presence of a small amount of a complex forming agent (EDTA) both Zn and its alloys dissolve. According to results presented in earlier works,[15,23] the best peak resolution was obtained for Zn–Ni deposits of 5 μm thickness, so deposits of this thickness were also investigated in this work. Zn–Ni alloys were deposited using the reverse current parameters given in Tables I and II. In all experiments, the average current density was 20 mA cm^{-2}. The phase structure of a Zn–Ni alloy deposited with a direct current of 20 mA cm^{-2} was also investigated.

The anodic linear sweep voltammograms obtained (Figs. 8 and 9) show the phase structures of Zn–Ni alloys desposited with a constant and reverse current density using different reverse plating parameters. The dissolution voltammogram of the alloy deposited by DC is shown by a solid line in Figs. 8 and 9.

On the basis of the ALSVs, the chemical composition and the equilibrium phase diagram of the Zn–Ni system,[24] an identification of the phase structures present in the Zn–Ni alloys obtained was made. A Zn–Ni alloy consists of several intermediate phases and/or intermetallic compounds of different crystallographic orientations. According to the equilibrium phase diagram,[24] the homogenous range between 76–77 mol % Zn corresponds to the γ_1-phase, a Zn content of 82–86

mol % corresponds to the γ-phase, and 89 mol % Zn to the δ-phase. According to some authors,[11] there is also a η-phase, which is a solid solution of Ni in Zn, with up to 1 mol % Ni.

After an anodic sweep of the Zn–Ni alloys with a Ni content above 20 wt. %, the deposit residues were observed on a RDE, and they could be mechanically removed easily. For certain RC parameters and when dissolution during t_a was significant (either in the case of the high current density amplitude, or a relatively long period of anodic dissolution, t_a) the alloy deposit was not compact, which explains the poor adhesion and deposit delamination during ALSV. Hence, the voltammograms obtained in these cases could not be used for the determination of the phase content of a Zn–Ni alloy.

The dissolution of the Zn–Ni alloy deposited by RC with $T = 0.1$ and 0.2 s (Fig. 8a) takes place under two voltammetric peaks, hence a two phase alloy was obtained, with the γ-phase prevailing. The anodic current peaks at potentials of –180 mV and –230 mV (Fig. 8c) correspond to the dissolution of the γ-phase, and the dissolution of this phase occurs after the dissolution of the δ-phase, characterized by shoulders at –350 mV and –450 mV.

On the basis of the chemical content of the Zn–Ni alloys deposited by RC with $r = 0.5$ and $T = 1$, 2 and 3 s (32, 39 and 42 mol % Ni, respectively) and the equilibrium phase diagram[24] it could be expected that the deposited Zn–Ni alloys would have two phases, but, as can be seen from Fig. 8b, there is only one ALSV dissolution peak, indicating the presence of only one phase. These results are in accordance with literature data,[25] according to which electrochemically deposited Zn–Ni alloys with 30 % Ni are made up of only the γ-phase, which was also verified by XRD.

The dissolution peak for Zn–Ni alloys deposited by RC with $T = 1$, 2 and 3 s (Fig. 8b) is in the potential range corresponding to the disolution of the γ-phase. With increasing T, the anodic peak shifts in the positive direction, indicating an increase in the content of the nobler component of the alloy, $i.e.$, Ni. This is in accordance with the previously shown results of chemical analysis, according to which an increase of T results in an increase of the Ni content of the alloy.

For $T = 5$, 10 and 20 s (Fig. 8c), there is also one voltammeric peak on the ALSVs at potentials corresponding to the dissolution of the γ-phase. With increasing T at a constant value of r, the anodic dissolution time, t_a, is also increased, hence a less compact deposit could be expected. As a consequence, there was partial delamination of the deposit during ALSV recording and a smaller voltammetric peak was obtained at larger T values (Fig. 8c), indicating the dissolution of only the part of the alloy having good adhesion.

The influence of the r value on the number and shape of the voltammetric peaks for Zn–Ni alloys deposited by RC with a constant $T = 1$ s is illustrated in Fig. 9a. The dissolution of these Zn–Ni deposits occurs under one voltammetric peak,

corresponding to γ-phase dissolution. The smaller height of the current peak for $r =$ 0.83 could be explained by delamination of the deposit during ALSV recording. For the Zn–Ni alloy obtained with $r = 0.5$, there is also only one voltammetric peak, but the higher Ni content in this alloy caused a shift of this peak potential to a more noble value.

A completely different peak/phase structure for Zn–Ni alloys deposited by RC with smaller r values was obtained (Fig. 9b). For small r values, when dissolution of Zn during the anodic time, t_a, could be neglected, the Zn–Ni deposits are characterized by two voltammetric peaks (Fig. 9b), which is in accordance with the phase structure of the alloy which would be expected based on the chemical content and the phase diagram. The peak current with the more noble peak potential (–230 mV) corresponds to γ-phase dissolution, while the one with the less noble peak potential (–460 mV) corresponds to δ-phase dissolution. For $r = 0.4$, the amount of δ-phase in the Zn–Ni alloy was calculated to be 30 %, from the ratio of the area under the less noble current peak to the overall area of the ALSV peaks, obtained by integrating the peaks in Fig. 9b. With a further decrease of r ($r = 0.33$ and 0.2, Fig. 9b), the amount of the zinc rich δ-phase increases to 42 % and 58 %, respectively. This is in accordance with the previously presented results of the chemical analyses, which indicated an increase of the Zn content with the decreasing r. It can be seen that the ALSVs of deposit obtained by RC and $r = 0.2$ is approaching the ALSV of the deposit obtained by DC, which could be expected since Zn dissolution could be neglected for small r values (short period of anodic dissolution, t_a, during RC plating).

Corrosion properties of Zn–Ni alloys

The Zn–Ni alloys were electrodeposited on steel panels by RC with different T and r values, as well as by DC ($j = 20$ mA cm^{-2}), as a reference. The average current density in the RC depositions was the same for all deposits, 20 mA cm^{-2}. The thickness of the deposits was 10 μm. The plated specimens were immersed in a 3 % aqueous NaCl solution and the open circuit potential (E_{ocp}) was measured daily, in order to investigate the corrosion resistance of the Zn–Ni deposits.

Electrodeposited zinc alloys act as sacrificial electrodes, meaning that they corrode preferentially, thus protecting the steel from corrosion. If an alloy has a high enough zinc content it could still have a more negative potential than steel and be more stable than a pure zinc coating. The corrosion stability of Zn–Ni alloys depends mainly on the Ni content.[7]

In the first set of experiments, Zn–Ni alloys were deposited with a constant r value ($r = 0.5$) and different values of T. The time dependence of E_{ocp} for steel plated with Zn–Ni alloys deposited with constant current and reverse current is shown in Fig. 10. The open circuit potential of a bare steel surface in 3 % NaCl was –640 mV *vs*. SCE and it is marked with a solid line in Fig. 10. Visually, it could be seen that steel panels with Zn–Ni deposits obtained with $T = 1$, 2 and 3 s were destroyed first.

These deposits are rich in Ni, and they were destroyed after only one day of exposure to NaCl solution. This is in agreement with literature data according to which Zn–Ni alloys with a high Ni content have a tendency to form pits and are destroyed easily due to pitting corrosion.[26] However, Zn–Ni alloys deposited with $T = 0.1$ and 0.2 s were destroyed after 96 and 72 h, respectively. Although, due to the higher Zn content, the values of E_{ocp} for Zn–Ni alloys deposited by RC with $T = 0.1$ and 0.2 s are slightly more negative than steel E_{ocp}, and a better corrosion stability would be expected, they were destroyed after only 96, or 72 h, which is a consequence of the deposits being non-compact. Thus, all the Zn–Ni deposits investigated in the first set of experimetns showed poor corrosion stability.
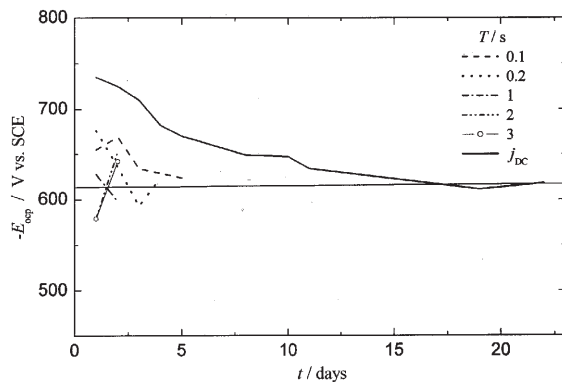

Fig. 10. The dependence of E_{ocp} for Zn–Ni alloys deposited on steel by RC with different reverse current wave periods, T, for a constant r value of 0.5.

In the second set of experiments, Zn–Ni alloys were deposited with a constant T value ($T = 1$ s) but with different values of r (Fig. 11). For $r = 0.83$ and 0.67, the deposits showed poor corrosion stability. After only a few hours of immersion in NaCl solution they turned yellow, as a consequence of the presence of Fe^{3+} ions. These deposits were also destroyed after only 24 h as well as a deposit obtained with $r = 0.5$. Due to high Ni content, the E_{ocp} values of these deposits are more positive than that of steel. However, deposits obtained with $r = 0.4$, 0.3 and 0.2 have higher Zn contents, hence the E_{ocp} values are more negative than that of steel, and thus these deposits could provide cathodic steel protection.
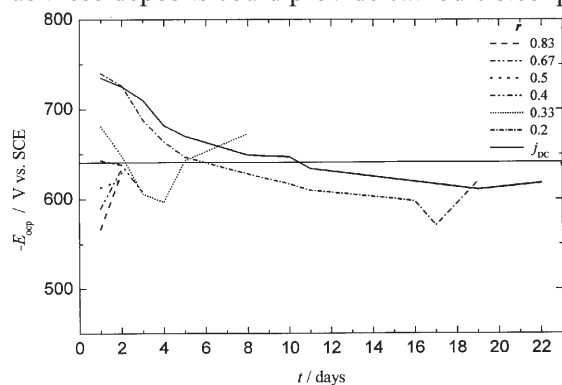

Fig. 11. The dependence of E_{ocp} for Zn–Ni alloys deposited on steel by RC with different r values, at a constant T value of 1 s.

The results of the visually observed alloy destruction in 3 % NaCl solution, or the appearance of red rust on the steel base, are presented in Table III.

TABLE III. The time of red rust appearance for Zn–Ni alloys deposited by RC with different r values, at a constant T value of 1 s.

r	0.40	0.33	0.20	0
t/h	48	120	456	528

On the basis of all these results it could be concluded that in RC plating with a constant T value, Zn–Ni alloys with better corrosion stability were obtained with smaller r values. Hence, the RC plating should be performed using small r values, *i.e.*, with a short anodic time duration, t_a in order to decrease Zn dissolution. By RC plating with small r values it is possible to obtain Zn–Ni alloys with the same chemical content and phase structure as with DC plating, but due to the anodic dissolution during t_a RC wave, the deposits obtained by RC plating are more compact.[13,14]

The deposit obtained with direct current ($r = 0$) had the best corrosion properties. Thus, the Zn–Ni deposits obtained by RC plating with the parameters examined in this work showed reduced corrosion stability as compared with alloys deposited by DC.

CONCLUSIONS

On the basis of the results obtained and literature data it could be concluded that the parameters of the reverse current influence the chemical content of Zn–Ni alloys. With the RC parameters used in this work, Zn–Ni alloys with 14–70 wt. % Ni were obtained. The Ni content in the alloy increases with increasing T at constant r, whereas it decreases with decreasing r at constant T.

The current efficiency increases with increasing T at constant r, due to the small overpotential of hydrogen evolution on the Ni enriched alloy. On the other hand, the current efficiency increases with decreasing r, at constant T, as a result of the decreased Ni content and the lower rate of hydrogen evolution.

Zn–Ni alloys deposited by RC with Ni above 30 wt.% have only one phase, and the dissolution current peak shifts to positive potential values with increasing Ni content and corresponds to the dissolution potential of the γ-phase.

With decreasing r, the ALSVs of the deposits obtained by RC approach the ALSV of a deposit obtained by DC.

Of all Zn–Ni alloys investigated in this work, the one deposited with $T = 1$ s and $r = 0.2$ showed the best corrosion properties. RC plating should be performed using small r values, *i.e.*, with shortest anodic time duration, t_a, in order to decrease Zn dissolution.

И З В О Д

ЕЛЕКТРОХЕМИЈСКО ТАЛОЖЕЊЕ И КАРАКТЕРИЗАЦИЈА ЛЕГУРА ЦИНК–НИКАЛ ДОБИЈЕНИХ КОНСТАНТНОМ И РЕВЕРСНОМ СТРУЈОМ

ЈЕЛЕНА Б. БАЈАТ[1], АЛЕКСАНДРА Б. ПЕТРОВИЋ[2] и МИОДРАГ Д. МАКСИМОВИЋ[1]

[1]*Технолошко-металуршки факултет, п. пр. 3503, 11120 Београд и* [2]*Крушик акумулатори а.д., 14000 Ваљево*

Испитивани су хемијски састав и фазна структура легура Zn–Ni добијених применом различитих параметара електрохемијског таложења. Легуре су таложене на ротирајућој диск електроди и на челичним плочицама константном и реверсном струјом. Испитивани су параметри реверсне струје (катодне и анодне густине струје таложења, и њиховог времена трајања) на састав, фазну структуру и корозионе особине легура. Показано је да хемијски састав и фазна структура утичу на корозионе особине Zn–Ni легура током излагања дејству раствора 3 % NaCl. Легура Zn–Ni добијена реверсном струјом са $T = 1$ s и $r = 0.2$ има најбоље корозионе особине.

REFERENCES

1. R. Fratesi, G. Lunazzi, G. Roventi, in *Organic and Inorganic Coatings for Corrosion Prevention*, L. Fedrizzi, P. L. Bonora, Eds., EFC Publication No. 20, The Institute of Materials, London, 1997, p. 130
2. S. R. Rajagopalan, *Met. Finish.* **70** (1972) 52
3. M. Pushpavanam, S. R. Natarajan, K. Balakrishnan, L. R. Sharma, *J. Appl. Electrochem.* **21** (1991) 642
4. M. A. Pech-Canul, R. Ramanauskas, L. Maldonado, *Electrochim. Acta* **42** (1997) 255
5. W. Kautek, M. Sahre, W. Paatsch, *Electrochim. Acta* **39** (1994) 1151
6. D. E. Hall, *Plat. Surf. Finish.* **70** (1983) 59
7. L. Felloni, R. Fratessi, E. Quadrini, G. Roventi, *J. Appl. Electrochem.* **17** (1987) 574
8. Y. Lin, J. R. Selman , *J. Electrochem. Soc.* **140** (1993) 1299
9. Y. Lin, J. R. Selman, *J. Electrochem. Soc.* **140** (1993) 1304
10. R. D. Srivastava, R. C. Mukerjee, *J. Appl. Electrochem.* **6** (1976) 321
11. S. Swathirajan, *J. Electrochem Soc.* **133** (1986) 671
12. S. Swathirajan, *J. Electroanal. Chem.* **221** (1987) 211
13. K. I. Popov, M. D. Maksimović, in *Modern Aspects in Electrochemistry,* B. E. Conway, J.O'M. Bockris, R. E. White, Eds., Vol. 19, Plenum Publishing Corporation, 1989, pp. 193–250
14. A. M. Pesco, H. Y. Che, in *Modern Aspects in Electrochemistry*, B. E. Conway, J.O'M. Bockris, R. E. White, Eds., Vol. 19, Plenum Publishing Corporation, 1989, pp. 251–293
15. J. B. Bajat, M. D. Maksimović, V. B. Mišković-Stanković, S. Zec, *J. Appl. Electrochem.* **31** (2001) 355
16. R. Fratesi, G. Roventi, *J. Appl. Electrochem.* **22** (1992) 657
17. D. Pletcher, *Industrial Electrochemistry*, Chapman and Hall, London, 1982
18. S. K. Gogia, S. C. Das, *J. Appl. Electrochem.,* **21** (1991) 64
19. V. D. Jović, R. M. Zejnilović, A. R. Despić, J. S. Stevanović, *J. Appl. Electrochem.* **18** (1988) 511
20. J. S. Stevanović, V. D. Jović, A. R. Despić, *J. Electroanal. Chem.* **349** (1993) 365
21. J. Stevanović, L. Skibina, M. Stefanović, A. Despić, V. Jović, *J. Appl. Electrochem.* **22** (1992) 172
22. S. K. Zečević, J. B. Zotović, S. Lj. Gojković, V. Radmilović, *J. Electroanal. Chem.* **448** (1998) 245
23. J. B. Bajat, M. D. Maksimović, G. R. Radović, *J. Serb. Chem. Soc.* **67** (2002) 625
24. D. A. Porter, K. A. Easterling, *Phase Transformations in Metals and Alloys,* Van Nostrand Reinhold Co. Ltd., Wokingham, 1980
25. R. Char, S. R. Panikkar, *Electroplating and Metal Finishing* (1960) 405
26. R. Albalat, E. Gomez, C. Muller, J. Pregonas, M. Sarret, E. Valles, *J. Appl. Electrochem.* **21** (1991) 44.